

# Anomalous phase transition in dipalmitoylphosphatidylethanolamine/palmitoylphosphatidylcho- line/water system

Carmelo La Rosa <sup>a,\*</sup>, Domenico Grasso <sup>a</sup>, Andrea Checchetti <sup>b</sup>, Attilio Golemme <sup>b</sup>,  
Giuseppe Chidichimo <sup>b</sup>, Phill Westerman <sup>c</sup>

<sup>a</sup> Dipartimento di Scienze Chimiche, Università di Catania, V. le A. Doria 6, 95125 Catania, Italy

<sup>b</sup> Dipartimento di Chimica, Università della Calabria, 87036 Arcavacata di Rende (CS), Italy

<sup>c</sup> Department of Biochemistry, Northeastern Ohio Universities College of Medicine, P.O. Box 95, Rootstown, OH 44272, USA

Received 24 February 1997; revised 22 May 1997; accepted 4 June 1997

## Abstract

An anomalous phase transition with a marked rise in specific heat, the isobaric thermal expansion coefficient, and the compressibility coefficient at 62.5°C for an equimolar mixture of 1,2-dipalmitoyl-*sn*-glycero-3-phosphoethanolamine (DPPE) and 1-palmitoyl-*sn*-glycero-3-phosphocholine (PLPC), in water (34 wt.%) has been shown by differential scanning calorimetry, scanning dilatometry and isothermal compressibility measurements. This transition occurs 15°C above a first-order transition observed in the same system. <sup>31</sup>P and <sup>2</sup>H nuclear magnetic resonance results are consistent with the occurrence of 'defects' in the bilayer in the temperature range between the first and the anomalous phase transitions. It is proposed that conically, PLPC molecules prefer regions with high curvature in the defective bilayer, while DPPE molecules are mostly confined to the flat regions of the bilayers. © 1998 Elsevier Science B.V.

**Keywords:** Phospholipid; Phase transition; DSC; Volumetric; NMR

## 1. Introduction

Amphipathic lipids self-assemble into several supramolecular structures when mixed with water [1–3]. An attempt to quantify the aggregation process and rationalize the formation of different assemblages has been made by Israelachvili et al. [4,5]. The following simple concept emerged: from this

theoretical model, the shape of the amphiphile greatly influences aggregate geometry.

Cylindrical-shaped lipids, such as phosphatidylcholines (PC) and phosphatidylethanolamines (PE), favor a planar bilayer, but lipids with a conical or wedge-like shape, such as lysophosphatidylcholine (lyso PC), tend to form micellar and cylindrical phases [6]. Cylindrical-shaped lipids that form bilayer aggregates may undergo a phase transition at a well-defined temperature ( $T_m$ ). Below this temperature, the hydrocarbon chains are arranged in an orderly crystalline lattice where the chains are in all

\* Corresponding author. Fax: +39-95-580138; e-mail: clarosa@dipchi.unict.it

*trans*-conformation. This phase is commonly referred as to the gel state. Above  $T_m$ , the hydrocarbon chains melt and are in a more disordered, liquid-like state, with a *gauche* conformation in the chains. This phase is commonly referred to as the liquid crystalline state. The magnitude of  $T_m$  depends on the nature of hydrocarbon tails, the polar region of the liquids, the amount of water present, and the solutes dissolved in water. Melting is a cooperative process that involves the collapse of the crystal lattice [7,8]. The destruction of microscopic regions of the lattice induces instability in the neighbouring regions, which break down and create new sources of instability. In single lipids, experimentally determined peaks for thermodynamic parameters such as isobaric specific heat, isothermal compressibility, and the isobaric expansion coefficient for the gel-to-liquid crystalline transition appear as being sharp and narrow. In contrast, the corresponding peaks for binary mixtures appear as the superposition of two or more broad peaks for miscible lipids and narrow peaks for immiscible lipids [9].

There has been recently increased interest in the supramolecular structures formed by mixtures of LPC with cylindrical-shaped lipids, because of the possible role such structures may play in membrane fusion and other biological processes [10–12]. Although the mechanism of the effect of LPC on membrane phospholipids remains unknown, its action probably results from specific interactions between hydrophilic headgroups and the different spatial requirements of the two types of lipids. To define the nature of these interactions more clearly, LPC/PC binary mixtures have been examined using several physical techniques [13–22]. The results of such study led the authors to conclude that the effect of LPC on lipids was highly complex depending on the length of the fatty acyl chains of both phospholipid and lysolecithin and that relatively small amounts of lysolecithin have a pronounced influence on the phase transition of pure lipids and on the miscibility of different phospholipids [22]. In contrast to LPC/PC mixtures, LPC/PE systems have received much less attention [23,24]. This paper presents the characterization of an equimolar mixture of 1,2-dipalmitoylphosphatidylethanolamine (DPPE) and 1-palmitoyllysophosphatidylcholine (PLPC), in water (34 wt.%) by differential scanning calorimetry

(DSC), scanning dilatometry (SD) and isothermal compressibility measurements. Our observations are worthy of notice because this system undergoes an anomalous phase transition at 62.5°C with continuous thermodynamic quantities such as enthalpy ( $H$ ) and volume ( $V$ ), and no latent heat. Isobaric specific heat, the isobaric expansion thermal coefficient and the isothermal compressibility coefficient have, in contrast, shown discontinuities [25]. The events occurring in the vicinity of this transition were studied by  $^{31}\text{P}$  and  $^2\text{H}$  nuclear magnetic resonance (NMR) to measure changes in orientational ordering at selected sites in two lipid components. The observed changes are explained in terms of the different shapes of the two lipid components, with the more conical PLPC probably preferring regions of high curvature in defective structures and the cylindrically-shaped DPPE confined to the flat regions of the bilayer.

## 2. Material and methods

### 2.1. Sample preparation

Samples were prepared by dissolving appropriate quantities of the dry lipids in a minimum amount of chloroform/methanol (95/5, v/v). The solvent was evaporated in vacuo, and the residue dried under high vacuum for 24 h. The necessary amount of water to give a final concentration of 34 wt.% was mixed with the lipid in a 7.5-mm glass tube. The tube was flame-sealed and the contents mixed above the main phase transition temperature until homogeneity was achieved. This process usually took about a day. DPPC- $d_9$  was prepared from DPPE by *N*-methylation using deuteriomethyl iodide (Aldrich, Milwaukee, WI) [26]. The 2-palmitoyl moiety was removed from DPPC- $d_9$  by treatment with phospholipase  $A_2$  using the method set out Keough and Davis [27], to yield 1-palmitoyllysophosphatidylcholine.

### 2.2. Differential scanning calorimetric measurements

DSC scans were carried out with a Setaram (Lyon, France) micro differential scanning calorimeter (microDSC) with 1 ml stainless steel sample cells, interfaced with a Bull 200 Micral computer. The

sampling rate was 1 point/s in all measuring ranges. Both the sample and reference (empty cell) were scanned from 30 to 80°C with a precision of 0.08°C. The calorimetric scans were performed at a nitrogen pressure of 1.5 bar.

To obtain the  $C_p$  curves, the base lines were obtained at the same scanning rate and then subtracted from sample curves. All the  $C_{p,exc}$  curves were obtained using a fourth-order polynomial fit. The average level of noise was about 0.4  $\mu$ W and reproducibility at refilling was about 0.1 mJ K<sup>-1</sup> ml<sup>-1</sup>.

Energy calibration was performed using a defined power supply, electrically generated by an EJ2 Setaram Joule calibrator within the sample cell.

### 2.3. Scanning dilatometric measurements

A Mettler TC10A processor equipped with a TMA thermomechanical analyser, previously calibrated for temperature and length was used to obtain measurements of length as a function of temperature at constant pressure. A quartz cylinder with a tight but freely movable piston was used as sample holder. The movement of the piston was measured as a length change of the sample. The scanning dilatometer, in the configuration described in Ref. [28], has a sensitivity of about  $3.2 \times 10^7$  ml reproducibility and 0.2% reproducibility. The deviation from linearity of the baseline in scanning conditions was less than 0.1%. Further details are reported in Refs. [29,30].

### 2.4. Isothermal compressibility measurements

Compressibility measurements were performed using a force measuring probe ranging from 0.0 to 1.35 N. Since the area of the piston was 3.801 mm<sup>2</sup>, the pressure extended on the sample varied from 1 to 4 atm. Further technical details are described in Ref. [30].

### 2.5. Nuclear magnetic resonance measurements

Spectra were obtained on an MSL 300 Bruker NMR spectrometer equipped with a variable temperature unit. Temperatures are correct to within  $\pm 0.5^\circ\text{C}$ . A Hahn echo sequence was employed for data acquisition. For the <sup>31</sup>P-NMR spectra a  $\pi/2$

pulse width of 2 ms was used with proton decoupling. The delay between the  $\pi/2$  pulse and the  $p$  pulse in the echo sequence was 40 ms and the repetition rate was 3 s. A quadrupolar echo sequence with a  $\pi/2$  pulse width of 3.5 ms was used for acquiring <sup>2</sup>H-NMR spectra. The delay between the two  $\pi/2$  pulses was 40 ms and repetition was 1 s. To allow samples to reach thermal equilibrium, spectra were recorded 30 min after each temperature change.

## 3. Results

### 3.1. Thermodynamic data

Thermodynamic data was obtained with the techniques described above, using scanning rates of 0.5°C/min. Other measurements at different scanning rates were carried out but are not presented.

Fig. 1 shows the temperature dependencies of specific heat ( $C_p$ ), the specific volume ( $V_s$ ), the expansion coefficient

$$\alpha = \frac{1}{V} \left( \frac{\partial V}{\partial T} \right)_P \quad (1)$$

and the isothermal compressibility coefficient

$$\beta = \frac{1}{V} \left( \frac{\partial V}{\partial P} \right)_T \quad (2)$$

for an equimolar mixture of DPPE and PLPC in H<sub>2</sub>O (34 wt.%).

With increasing temperature,  $C_p$ ,  $\alpha$  and  $\beta$  shows a sharp peak at 47.3°C ( $\Delta H$  of 3.16 kcal/mole), followed by a slow, monotonic increase in value over a range of about 15°C. The relative specific volume change at 47.3°C ( $\Delta V/V_s$ , %) is 2.2%, whereas it is zero at 62.5°C. Other experiments at different scanning rates (from 0.016 to 1°C/min) were also performed. Decreasing the scanning rate causes  $T_m$  to decrease in an exponential fashion to a temperature approximately 3°C lower.  $\Delta H$  remains quite constant in both the heating and cooling modes. In the cooling mode a hysteresis in the transition at 47.3°C was the only thing to be observed, while the transition at 62.5°C did not appear. The hysteresis vanished if the scanning rate was set very low

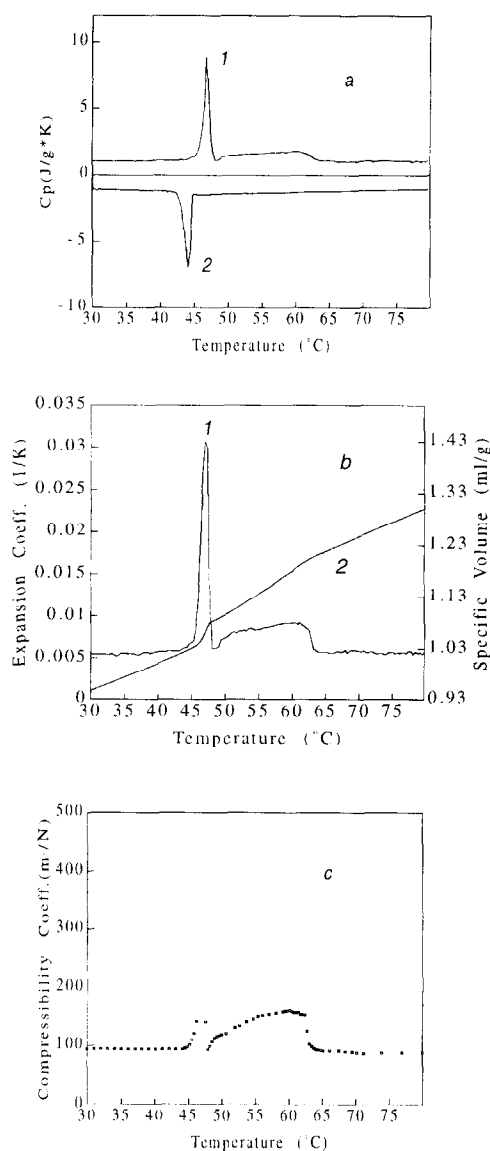


Fig. 1. Thermodynamic functions as a function of temperature for an equimolar mixture of DPPE/PLPC in water (34 wt.%). (a) Isobaric specific heat: 1-heating, 2-cooling; (b) isobaric expansion coefficient (1) and specific volume (2); (c) isothermal compressibility.

(0.016°C/min). The transitions observed (Fig. 1) are completely reproducible when scanning the same sample more than once, and are therefore totally reversible.

An interesting function that can be obtained from isothermal compressibility measurements is the mean fluctuation of the volume in a phase. The volume

fluctuation  $\langle V \rangle^2$  is given by [31]

$$\langle V \rangle^2 = -T \left( \frac{\partial V}{\partial P} \right)_T \quad (3)$$

where  $T$  is the absolute temperature and  $(\partial V/\partial P)_T$  is isothermal compressibility. The following refer to one mole:

$$\langle V \rangle^2 = V_m \beta_T kT \quad (4)$$

where  $k$  is the Boltzmann constant and  $V_m$  the molar volume. The rms volume fluctuation together with  $\beta$ , the molar volume ( $V_m$ ),  $\Delta V_{rms}$  and the relative  $\Delta V_{rms}\%$  ( $\Delta V_{rms}/V_m \times 100$ ) at various temperatures are shown in Table 1. We note that the rms fluctuations in the range from the transition at 47.3°C to the transition at 62.5°C, are very high compared with those at temperatures below 47.3°C and above 62.5°C. Moreover, the compressibility coefficient and fluctuations in DPPE/PLPC compared to DPPE ( $\beta = 55.8 \times 10^{-11} \text{ m}^2/\text{N}$ ,  $\Delta V_{rms} = 30.96 \text{ cm}^3$  measured at 35°C and  $\beta = 71.4 \times 10^{-11} \text{ m}^2/\text{N}$ ,  $\Delta V_{rms} = 43.1 \text{ cm}^3$  measured at 70°C [32]) are also very high. Although the fluctuations, from compressibility data and other thermodynamic quantities is a bulk thermodynamic property, it could provide important information on the microscopic states in a phase, in combination with the data obtained from X-ray and nuclear magnetic resonance analyses. Such volume fluctuations appear to result predominantly from the imperfect atomic packing and the dynamic-domain character of the phospholipid molecules in the bilayer. Thus, the packing of the DPPE/PLPC system in the temperature range from 47.3 to 62.5°C contains more 'defects' compared to its gel and liquid crystal phases.

According to Ehrenfest's [31] classification of phase transitions, when the molar Gibbs free energy ( $G$ ) is a continuous function and its first derivative with respect to temperature  $(\frac{\partial G}{\partial T})_P = -S$  is discontinuous, the transition is defined as being first-order. Instead, when  $G$  and  $(\frac{\partial G}{\partial T})_P = -S$  are continuous and  $(\frac{\partial^2 G}{\partial T^2})_P = -C_p$  is discontinuous, the transition is defined as a second-order phase transition [31,33]. Therefore, in a first-order phase transition enthalpy, entropy and volume show a change at the transition temperature and its first derivatives  $C_p$ ,  $\alpha$  and  $\beta$  tend towards infinity. In a second-order phase transition, changes in enthalpy, entropy and volume at the

Table 1

Isothermal compressibility coefficients ( $\beta \times 10^{11}$ ,  $\text{m}^2/\text{N}$ ), molar volumes ( $V_m$ ,  $\text{cm}^3/\text{mole}$ ), volume fluctuations ( $\Delta V_{\text{rms}}$ ,  $\text{cm}^3/\text{mole}$ ) and relative volume fluctuation  $\Delta V_{\text{rms}}\%$  ( $\Delta V_{\text{rms}}/V_m \times 100\%$ ) at several temperatures for DPPE/PLPC/ $^2\text{H}_2\text{O}$  (41/25/34 wt.%)

$T$ ( $^{\circ}\text{C}$ )	$\beta$	$V_m$	$\Delta V_{\text{rms}}$	$\Delta V_{\text{rms}}\%$
35	93.42	671.00	40.0	5.96
50	118.75	796.86	50.4	6.32
55	150.81	827.13	58.3	7.05
60	160.31	868.93	62.7	7.21
65	91.04	890.62	47.7	5.35
70	87.08	913.29	47.6	5.21

transition temperature do not occur, its first derivatives show a change in value.

Fig. 1 shows clearly that the transition at  $47.3^{\circ}\text{C}$  is a first-order phase transition, whereas the transition at  $62.5^{\circ}\text{C}$  is anomalous and would appear to be a second-order phase transition since  $\Delta H = 0$  and  $\Delta V = 0$ , while  $C_p$ ,  $\alpha$  and  $\beta$  show a change in value. A change in symmetry is required when a second-order phase transition occurs [31].  $^{31}\text{P}$ - and  $^2\text{H}$ -NMR experiments were performed to determine which molecules between two phospholipids are involved in the symmetry change.

### 3.2. Spectroscopic data

$^{31}\text{P}$ - and  $^2\text{H}$ -NMR are techniques that are sensitive to the state of aggregation of phospholipids in water [34,35]. The phospholipids in a bilayered structure typically give rise to a broad asymmetric  $^{31}\text{P}$ -NMR spectrum with a low frequency shoulder [34]. In contrast, a hexagonal or cylindrical arrangement of phospholipids usually produces a narrower spectrum that is approximately half the width of the corresponding lamellar phase, and displays a high-frequency shoulder. The spectral lineshape is determined by the principal components of the chemical shift tensor modulated by the motions of the phosphorus nucleus. The residual chemical shift anisotropy (CSA),  $\Delta\sigma = \sigma_{\parallel} - \sigma_{\perp}$  may readily be evaluated from the singular positions of the spectral edges and is a measure of the orientations and time-average fluctuations of the phosphate segment in a phospholipid.

$^{31}\text{P}$ -NMR spectra of a DPPE/PLPC/ $^2\text{H}_2\text{O}$  (41/25/34 wt.%) mixture recorded at various temperatures are shown in Fig. 2a. At  $T = 35^{\circ}\text{C}$  below

the first-order transition, the spectrum has a line-shape that is characteristic of a lamellar phase in the gel state with a CSA of about 4.5 kHz. At  $T = 50^{\circ}\text{C}$  (just above the first-order phase transition), the spectra are the superposition of two powder patterns: one arising from the lamellar phase and the other from a cylindrical phase with a CSA about one-half of the magnitude of the lamellar phase, but with its oppo-

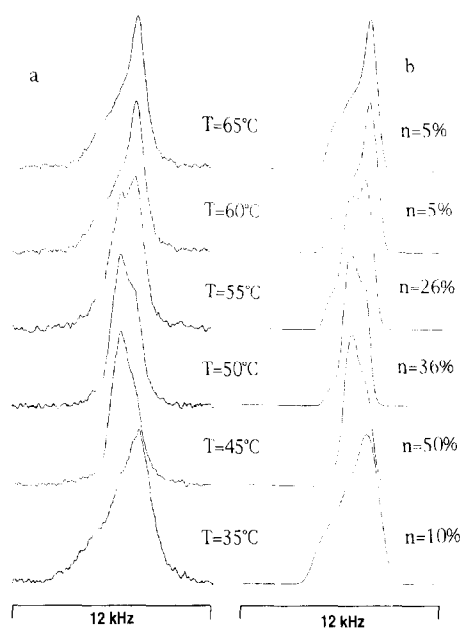


Fig. 2. (a)  $^{31}\text{P}$ -NMR spectra of DPPE/PLPC/ $^2\text{H}_2\text{O}$  (41/25/34 wt.%) dispersions recorded at 121.26 MHz at different temperatures. (b) Theoretical fits of  $^{31}\text{P}$ -NMR spectra for the DPPE/PLPC/ $^2\text{H}_2\text{O}$  system at different temperatures.  $n$  is the mole percentage of phosphorus segment with cylindrical symmetry used in the simulations.

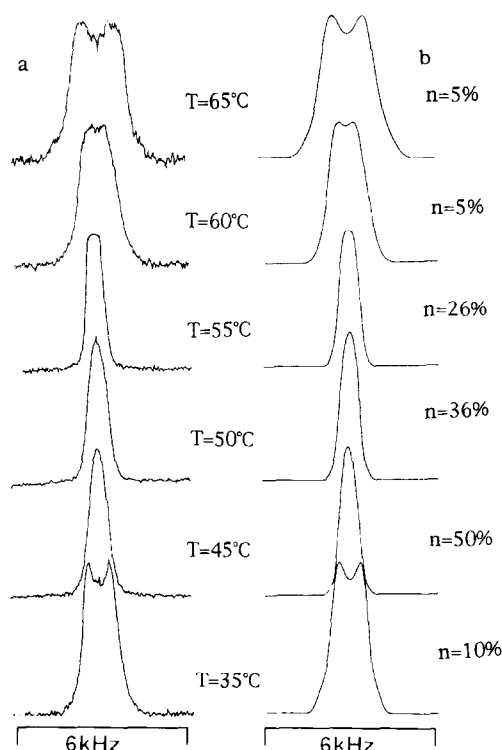


Fig. 3. (a)  $^2\text{H}$ -NMR spectra of DPPE/PLPC/ $^2\text{H}_2\text{O}$  (41/25/34 wt.%) dispersions recorded at 46.53 Mhz at different temperatures. (b) Theoretical fits of the  $^2\text{H}$ -NMR spectra for the DPPE/PLPC/ $^2\text{H}_2\text{O}$  system at different temperatures.  $n$  is the mole percentage of water molecules adopting a with cylindrical symmetry used in the simulations.

site sign. The CSA of the lamellar powder pattern is slightly narrower than the pattern observed at  $T = 35^\circ\text{C}$ . The relative intensity of signals from the lamellar phase increases along with temperature up to  $60^\circ\text{C}$  where the spectral pattern is indicative of an exclusively lamellar phase.

To gain further insight into the structural changes occurring at these transitions, we have performed  $^2\text{H}$ -NMR spectra of the DPPE/PLPC/ $^2\text{H}_2\text{O}$  system over the same temperature range. Representative spectra are shown in Fig. 3a. The spectrum recorded at  $35^\circ\text{C}$  appears as a uniaxial powder pattern with a splitting of about 900 Hz. This doublet collapses into a broadened singlet over the  $45$ – $60^\circ\text{C}$  range. The collapse of the uniaxial pattern is probably due to the rapid exchange of lipid-bound water molecules between phases with lamellar and cylindrical symme-

try. A uniaxial powder pattern characteristic of a lamellar phase reappears at temperatures above  $60^\circ\text{C}$ . This line shape occurs again even at these higher temperatures because diffusion along the surface of the lamellar phase is not sufficient alone to completely randomize the orientation of the  $^2\text{H}_2\text{O}$  molecules during NMR measurements [36].

Since the contribution of  $^{31}\text{P}$  nuclei in both DPPE and PLPC molecules to the spectral powder patterns in the  $^{31}\text{P}$ -NMR spectra may complicate their interpretation, we performed  $^2\text{H}$ -NMR experiments on the same mixture in which the PLPC molecules were  $^2\text{H}$ -labeled in the trimethylammonium moiety (PLPC- $d_9$ ). Spectra recorded at different temperatures are shown in Fig. 4. The right side of this figure shows enlarged views of several spectra shown on the left. The spectra, recorded below the first-order phase transition temperature ( $47.3^\circ\text{C}$ ), consist of a broad central signal superimposed on a Pake doublet. The quadrupole splitting of the Pake doublet de-

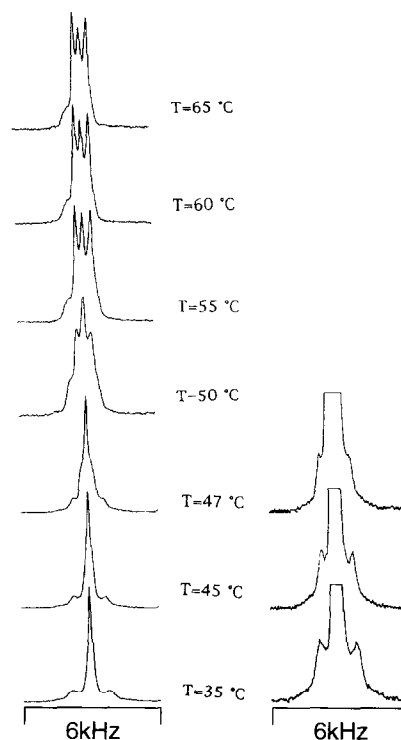


Fig. 4.  $^2\text{H}$ -NMR spectra of DPPE/PLPC- $d_9$ / $\text{H}_2\text{O}$  dispersions at different temperatures. Enlarged view of the low-temperature spectra are shown on the right.

creases from 1.6 to 1.2 kHz between 35 to 47°C. The central signal is broader and more prominent in the spectrum recorded at 47°C and was assigned to PLPC- $d_9$  molecules dispersed in DPPE. This spectral component resembles the spectrum of a PLPC- $d_9$ /water binary system in a hexagonal phase at comparable temperatures (data not shown). As temperature increases above 50°C, the central signal diminishes and a powder pattern ( $\Delta\nu \cong 1.6$  kHz), characteristic of a lamellar phase, appears (Fig. 4). At 65°C the spectrum consists predominantly of this powder pattern and of a small sharp central peak of unknown origin. This latter peak appears to be present throughout the whole temperature range examined.

The observed lineshape change of the broad central signal in the  $^{31}\text{P}$ -NMR spectra was correlated with concentration change in the percentage ( $n$ ) or mole fraction of phospholipid molecules with cylindrical symmetry by fitting the experimental  $^{31}\text{P}$ -NMR spectra (Fig. 2b) to simulated lineshapes. The chemical shift at a given resonance,  $\sigma(\theta_0)$ , is expressed with reference to isotropic position  $\sigma_1$  [37,38]:

$$\sigma_{\text{cyl.lam}}(\theta_0) = \frac{\nu_0 - \nu(\theta_0)}{\nu_0} - \sigma_1$$

$$= \frac{1}{3} \Delta\sigma_{\text{cyl.lam}} (3\cos^2\theta_0 - 1) \quad (5)$$

where  $\Delta\sigma_{\text{cyl.lam}}$  is the residual chemical shift anisotropy of the cylindrical and lamellar phases, respectively;  $\sigma_1$  is the isotropic chemical shift value; and  $\theta_0$  is the polar angle defining the direction of the external magnetic field in the aggregate reference frame.  $^{31}\text{P}$ -NMR spectra were generated by a linear combination of the powder patterns of the cylindrical and lamellar phases.

The spectral lineshapes were found to depend on the concentration,  $n$ , of phosphate segments with cylindrical symmetry, on two CSA parameters and on two broadening parameters.  $n$  is the main fitting parameter and could be determined with a precision of  $\pm 0.02$ . The dependence of  $n$  on temperature is shown in Fig. 5. Our model of the transition is supported by the close similarity between simulated and experimental spectra (Fig. 2). Phospholipid molecules with cylindrical symmetry are present at

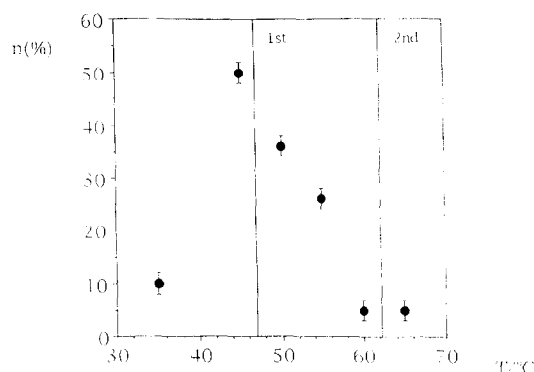


Fig. 5. Dependence of the mole percentage of phospholipids,  $n$ , with cylindrical symmetry as a function of temperatures. The two vertical solid lines indicate the temperatures at which the first- and the second-order phase transition occur.

all temperatures and show a significant increase in the first-order transition followed by a gradual decline to a value of 5 molar % over the course of the second-order transition.

The  $^2\text{H}$ -NMR spectra shown in Fig. 3 were fitted using similar methods. Assuming that  $^2\text{H}_2\text{O}$  molecules can sample all relevant orientations of the aggregate over measuring time, the spectral powder is given by the equation [39,40]:

$$\nu_{\pm} = \pm \frac{3}{4} \bar{\nu} \left[ \frac{3\cos^2\theta_0 - 1}{2} + \frac{\eta \sin^2\theta_0 \cos^2\phi_0}{2} \right] \quad (7)$$

where  $\nu_{\pm}$  are the intensities of individual frequencies for a given  $\theta_0$  and  $\phi_0$ ;  $\bar{\nu}$  is the partially averaged quadrupolar coupling constant;  $\theta_0$  and  $\phi_0$  are the polar and azimuthal angles defining the direction of the external magnetic field in the aggregate reference frame; and  $\eta$  is the asymmetry parameter, which is close to zero for uniaxial mesophases. It was found that experimental lineshapes could be generated using two quadrupole splitting parameters and a concentration parameter,  $n$ , which defines the fraction of phospholipids with cylindrical symmetry. A good fit between simulated and experimental spectra was obtained at comparable temperatures using

the same  $n$  values used in the fitting of the  $^{31}\text{P}$ -NMR spectra.

#### 4. Discussion

The following discussion of our interpretation of the above NMR and thermodynamic data is divided into four temperature regions: (i) 30–45°C; (ii) sharp transition; (iii) 51–65°C; (iv) above 65°C.

(i) In this lowest temperature range, the  $^{31}\text{P}$ -NMR data leads us to propose that there exist large near-planar lamellar structures in which PLPC and DPPE are mixed in the plane of the bilayer and equally distributed between the two monolayers of the bilayer. Most of the components of the hydrocarbon chain of both lipids are in *trans* configuration. At the same time a large network of ‘defects’ are spread throughout the bilayer, these sites being PLPC-enriched. Approximately 10% of the total lipid or 20% of the PLPC is found where defects occur, these resembling tears or pores in the fabric of the membrane. A dynamic situation with the continual breakage and reformation of defects may be envisaged.

(ii) At 47.3°C, where a first-order transition is observed, a major spatial segregation of the two lipid components occurs. We propose that this segregation is initiated by two related events. The first is the melting of the hydrocarbon chains of the PLPC molecules and the second, the segregation of PLPC and DPPE molecules to the opposite side of the bilayer. Evidence for the chain melting at 47.3°C is that there is a first-order transition at 32°C in the binary PLPC/water (34 wt.%) system which has comparable thermodynamic parameters (3.16 kcal/mole and 2.19 kcal/mole, respectively). Melting occurs at a higher temperature in the ternary system because each PLPC molecule in the gel state is surrounded by higher melting DPPE molecules rather than identical PLPC molecules in pure PLPC aggregates. The consequence of PLPC chain melting is the increased translational and transbilayer diffusion of the PLPC molecules leading to transbilayer segregation and a dramatic increase in the curvature of the bilayer. We propose that the bilayer is forced out of planarity and forms either much smaller multilamellar vesicles or tube-like structures. A precedent for the former structure exists in the ternary EPC/distearoylphosphatidylglycerol (DSPG)/water

system, whose,  $^{31}\text{P}$ -NMR [41] resembles the spectra observed in Fig. 2 between 47 and 40°C. It has been proposed that under certain conditions, this ternary exists as small multilamellar vesicles (diameter = 400 nm) with the larger, conically-shaped DSPG on the outside monolayer of the bilayer. Tube-like structures are an alternative explanation for the  $^{31}\text{P}$ -NMR data. Rapid lateral diffusion of PLPC around the outside of randomly oriented tubes would generate a powder pattern identical to that of a phase with cylindrical symmetry. It should be pointed out that several precedents exist for the asymmetric distribution of lysoPC across bilayers in aqueous dispersions of lipid mixtures. Chidichimo et al. [42] have shown that vesicles containing equimolar amounts of lysoPC and cholesterol are drastically asymmetric, and that lysoPC has a distinct preference for the outer bilayer shell. The same group also showed that lysoPC in highly curved POPC/lysoPC vesicles preferred the outer bilayer leaflet. Yet a third explanation of the molecular events occurring in the vicinity of the phase transition at 47.3°C, which does not cause segregation across the bilayer, is one that postulates increased segregation of PLPC molecules within the plane of the bilayer. Lateral migration of PLPC molecules could occur to create pores or breaks whose borders are PLPC-enriched. For the phase transition in this model it is necessary to postulate a large increase in the number of pore or ‘defective’ structures. In addition to the three models described above, it is possible that any combination of all three may account for the physical events occurring at the transition. Whatever the explanation, it is apparent that the structural changes occurring at 47.3°C provide additional opportunities for time-averaging the residual quadrupole splitting ( $\Delta\nu$ ) observed in the water molecule below 47.3°C. Simple diffusion across a bilayer surface does not average this quantity to zero, but the change to diffusion around a tubular surface, or around small multilamellar vesicles or through pore structures, reduces  $\Delta\nu$  to zero.

(iii) Increasing the temperature also results in the melting of the acyl chains of DPPE. The first population of DPPE molecules to experience an abrupt increase in the number of *gauche* conformations of its acyl chains are those molecules with the greatest number of neighbouring ‘melted’ PLPC molecules. Melting of the DPPE chain continues gradually with



increasing temperature until all its acyl chains are in a fluid state at approximately 63°C. During this process (if the system exists as a bilayer filled with pores), there is a lateral expansion that results in a decrease in the radii of the pores and ultimately in the formation of a large number of lattice defects. If the system exists as tubes or small MLVs, then chain melting probably increases molecular diffusion and the rate of diffusion of these macromolecular assemblages. In either case, the result is that of reestablishing a lamellar structure in which there are approximately equal populations of PLPC and DPPE molecules on each side of the MLV bilayers. The above models of a continuous phase transition are supported by the thermodynamic data that show a continuous volume change throughout the temperature range 50–63°C.

Moreover, Fig. 1 reveals that in cooling mode, any change in  $C_p$  between 63–50°C is observed at the same scan rate.  $C_p$  decreases in a straightforward manner. On the contrary, the first-order phase transition is shown with the usual scan rate-dependent hysteresis.

When a first-order phase transition takes place, the molecules are 'forced' by temperature stimulus to go from the lower energy state to the upper energy state. This transition is induced by heating the sample, and this energy is transformed into molecular motion (specific heat increase). When the system in the upper energy state is cooled, a relaxation occurs, lowering the energy level. The relaxation rate or decay rate is directly proportional to the coordination number (number of nearest neighbors) and to thermal conductivity. It is proportionally inverse to density and isobaric specific heat. Of course, since thermal conductivity is a function of temperature (and gradient), the molecules' heating and cooling pathways are different. From the above argument, we observe hysteresis in a first-order transition in the cooling mode, and an energy change is evident. In a second-order phase transition in which a continuous change in enthalpy and volume occurs (transition between energy states with equal or very nearly equal energies and different symmetries) only a straightforward slow decrease in  $C_p$ ,  $\alpha$  and  $\beta$  is observed.

(iv) In this temperature range, all lipids are in a lamellar liquid crystalline state with PLPC and DPPE

molecules intermixed. Again, diffusion of water across the bilayer surface alone is insufficient to time-average the quadrupole splitting.

Although we examined PLPC/DPPE mixture at six different molar ratios, only in the case of an equimolar mixtures was a second-order phase transition observed. To clarify the order of the anomalous transition, other experimental investigations using different techniques able to detect fast phenomenon, such as the phospholipid motions, are necessary.

These observations have both theoretical and biological significance. They are important theoretically because an equimolar PLPC/DPPE mixture represents a simple model for further study of second-order phase transitions in phospholipid/water dispersions.

Biologically, the formation of pores in membranes, produced by the association of PE with lysolecithin (arising from the action of phospholipase  $A_2$  on PC), may provide a mechanism for the non-mediated transport of ions across a normally impermeable lipid bilayer [2] or in the process of protein translocation [43–46].

## Acknowledgements

The technical support of Robin Jacquet is gratefully acknowledged. We thank Germano Iannacchione for helpful discussion. This research was supported with a grant from the American Heart Association, Ohio Affiliate and Italian MURST.

## References

- [1] V. Luzzati, *Biological Membranes*, in: D. Chapman (Ed.), Academic Press, New York, 1968, p. 37.
- [2] L. Rilfors, G. Lindblom, A. Weislander, A. Christiansson, *Membrane Fluidity*, in: M. Kates (Ed.), Plenum, 1984, p. 205.
- [3] S.M. Gruner, *The Structure of Biological Membranes*, in: P. Yagle (Ed.), CRC Press, Boca Raton, FL, 1991, p. 211.
- [4] J.N. Israelachvili, D.J. Mitchell, B.W. Ninham, *J. Chem. Soc., Faraday Trans. 2* 72 (1976) 1525.
- [5] J.N. Israelachvili, S. Marcelja, R.G. Horn, *Q. Rev. Biophys.* 13 (1980) 753.
- [6] G. Arvidson, I. Brentel, A. Khan, G. Lindblom, K. Fontel, *Eur. J. Biochem.* 152 (1985) 753.
- [7] J.F. Nagle, *Ann. Rev. Phys. Chem.* 31 (1980) 157.
- [8] E. Freire, R. Biltonen, *Biopolymers* 17 (1978) 481.

- [9] S. Mabrey, J. Sturtevant, *Proc. Natl. Acad. Sci. U.S.A.* 73 (1976) 3862.
- [10] R.D. Hoffman, M. Kligerman, T.M. Sunt, N.D. Anderson, H.S. Shin, *Proc. Natl. Acad. Sci. U.S.A.* 79 (1982) 3285.
- [11] M.T. Quinn, S. Parthasarathy, D. Stainberg, *Proc. Natl. Acad. Sci. U.S.A.* 85 (1988) 2805.
- [12] T. Saito, A. Wolf, N.K. Menon, M. Saeed, R.J. Bing, *Proc. Natl. Acad. Sci. U.S.A.* 85 (1988) 8246.
- [13] Y. Lee, S.I. Chan, *Biochemistry* 16 (1977) 1303.
- [14] D.A. Morris, R. McNeil, F.J. Castellino, J.K. Thomas, *Biochim. Biophys. Acta* 632 (1980) 380.
- [15] K. Elamrani, A. Blume, *Biochemistry* 21 (1982) 521.
- [16] A.D. Bangham, R.W. Horne, *J. Mol. Biol.* 8 (1964) 660.
- [17] H. Utsumi, K. Inoue, S. Nojima, T. Kwan, *Biochemistry* 17 (1978) 1990.
- [18] C.J.A. van Echteld, B. de Kruijff, J.G. Mandersloot, J. de Geir, *Biochim. Biophys. Acta* 649 (1981) 211.
- [19] D.M. Small, *J. Am. Oil Chem. Soc.* 45 (1968) 108.
- [20] B. de Kruijff, A.M.H.P. van den Besselaar, L.L.M. van Deenen, *Biochim. Biophys. Acta* 465 (1977) 443.
- [21] V.V. Kumar, B. Malewicz, W.J. Baumann, *Biophys. J.* 55 (1989) 789.
- [22] J.G. Mandersloot, F.C. Reman, L.L.M. van Deenen, J. de Geir, *Biochim. Biophys. Acta* 382 (1975) 443.
- [23] A. Blume, B. Arnold, H.U. Weltzien, *FEBS Lett.* 61 (1976) 199.
- [24] R.M. Eand, *Biochemistry* 24 (1985) 7092.
- [25] H.E. Stanley, *Introduction to Phase Transitions and Critical Phenomena*, Oxford Univ. Press, New York, 1971.
- [26] H. Eibl, *Chem. Phys. Lipids* 26 (1980) 405.
- [27] K.M.W. Keough, P.J. Davis, *Biochemistry* 18 (1979) 1453.
- [28] D. Grasso, *Liq. Cryst.* 2 (1987) 557.
- [29] D. Grasso, C. La Rosa, A. Raudino, F. Zuccarello, *Liq. Cryst.* 3 (1988) 1699.
- [30] C. La Rosa, D. Grasso, *Il Nuovo Cimento sez. D* 12 (1990) 1213.
- [31] L.D. Landau, E.M. Lifshits, *Statistical Physics*, Pergamon, London, 1975.
- [32] A. Raudino, F. Zuccarello, C. La Rosa, G. Buemi, *J. Phys. Chem.* 94 (1990) 4217.
- [33] I.P. Sugár, *J. Phys. Chem.* 91 (1987) 95.
- [34] I.C.P. Smith, I.H. Ekiel, *Phosphorus 31-NMR, Principles and Applications*, in: D. Gorestein (Ed.), Academic Press, London, 1984.
- [35] J.H. Davis, *Biochim. Biophys. Acta* 737 (1983) 117.
- [36] L.M. Strenk, P.W. Westerman, N.P.A. Vaz, J.W. Doane, *Biophys. J.* 48 (1985) 355.
- [37] A. Checchetti, G. Chidichimo, A. Golemme, C. La Rosa, D. Grasso, P.W. Westerman, *Chem. Phys. Lipids* 82 (1996) 147.
- [38] C.P. Schlichter, *Principles of Magnetic Resonance*, Harper and Row, New York, 1963.
- [39] M.A. Hemminga, P.R. Cullis, *J. Magn. Reson.* 47 (1982) 307.
- [40] G. Chidichimo, N.A.P. Vaz, Z. Yaniv, J.W. Doane, *Phys. Rev. Lett.* 49 (1982) 1950.
- [41] D.J. Phothinos, P.J. Bos, J.W. Doane, M.E. Neubert, *Phys. Rev. A* 20 (1979) 2203.
- [42] G. Chidichimo, A. Golemme, J.W. Doane, *J. Chem. Phys.* 82 (1985) 34.
- [43] D.M. Engelman, T.A. Steitz, *Cell* 3 (1981) 411.
- [44] M.A. Nesmeyanova, *FEBS Lett.* 142 (1982) 189.
- [45] G. von Heijne, *Eur. J. Biochem.* 103 (1980) 431.
- [46] W. Wickner, *Science* 210 (1990) 864.